Relaxation behaviour in the alpha beta splitting region of the glass transition in PnBMA by means of ^{13}C 2D-MAS exchange NMR

1995 J. Phys.: Condens. Matter 7 7419

(http://iopscience.iop.org/0953-8984/7/38/002)

J. Phys.: Condens. Matter 7 (1995) 7419–7426. Printed in the UK

Relaxation behaviour in the $\alpha\beta$ splitting region of the glass transition in PnBMA by means of ^{13}C 2D-MAS exchange NMR

W Domberger, D Reichert, F Garwe, H Schneider and E Donth
University of Halle, Department of Physics, D-06099 Halle/Saale, Germany

Received 12 May 1995

Abstract. Two distinct exchange rates are obtained in the splitting region of local (β) and cooperative (α) relaxations for poly(n butyl methacrylate) (PnBMA) by ^{13}C 2D-MAS exchange NMR. They fit well to the shear loss modulus traces of α and β in the Arrhenius diagram.

1. Introduction

The α (main) transition and the conventional β (secondary or local) transition are well known relaxations in amorphous polymers (McCrum *et al* 1967). A certain interrelation between them has long been suggested (Johari and Goldstein 1970), but detailed investigations of the splitting (as seen from high temperature) or merging (from low temperature) of their traces in an Arrhenius diagram are difficult, mainly because of the high frequencies $\geqslant 1$ MHz usually characteristic for this region. Recently poly(n alkylmethacrylates), especially PnBMA (butyl), have been investigated by dynamic shear and dielectric methods (Garwe *et al* 1994) since here the $\alpha\beta$ splitting region is in the Hz range, easily accessible to precise dynamic shear methods. In PnBMA a separate α onset (more than one decade below the β trace) was observed, in accordance with a scenario suggested by molecular simulations in a modified Fredrickson model (Schulz and Donth 1994). Moreover, the onset of the α shear loss modulus (G'') maximum is at lower temperatures than the dielectric onset. The G''_{max}, however, is at higher frequencies than the dielectric loss (ϵ'') maximum trace for $T < 35$ °C, but still lower than β.

Modern exchange NMR methods (Spiess 1991, Schmidt-Rohr *et al* 1994, Schmidt-Rohr and Spiess 1994) are also able to record relaxation rates in the Hz range. Such methods were applied to PEMA (ethyl) (Kulik *et al* 1994) with the aim of finding relevant molecular mechanisms for the β relaxation revealed by monitoring the molecular motion of the ^{13}C-labelled –COO– units. However, the use of ^{13}C-enriched samples and the focus on the β relaxation restricted these experiments to a relatively short time scale ($\leqslant 0.5$ s). A first indication for two distinct relaxation times was mentioned by the above authors.

The aim of this paper is a direct investigation of the $\alpha\beta$ splitting region in PnBMA by rotor-synchronized two-dimensional (2D) ^{13}C-NMR magic angle spinning (MAS) measurements. Compared to the static method used by Kulik *et al* (1994), this method has the advantages of high spectral resolution (almost all C atoms in the monomeric unit are resolved; cf the one-dimensional spectrum in figure 1), and high signal intensities (no ^{13}C enrichment is necessary). It will be shown that two distinct relaxation times can be observed that correspond to the exchange rates of two different processes. These relaxation times can

0953-8984/95/387419+08$19.50

be directly compared with the α and β relaxation times mentioned above. We expected to find these NMR times for the α-process near its G''_{max} trace, similarly to what is found for other amorphous polymers (PS, PVAC, PVC, PMMA) far below the splitting region (Donth *et al* 1979, Schneider and Donth 1986, Fedotov and Schneider 1989). It should be noted that the 2D-MAS experiment is less sensitive to the detailed molecular mechanism; however, it is well suited for revealing rate constants. Thus, in this contribution, we focused out attention on the determination of the characteristic time constants for the α and β processes and a comparison with other experimental techniques.

2. Sample preparation

The samples were purchased from Polyscience Inc. and measured as received. Several repeated measurements after large time intervals gave the same results, demonstrating that the experiments are thermoreversible. PnBMA has an average molecular weight $M_w = (330 \pm 8)$ kg mol^{-1} with $M_w/M_n = 2.35 \pm 0.1$ (determined by gel permeation chromatography (GPC) with a polystrene standard). The glass transition temperature $T_g = 24 \pm 2$ °C was calculated by an equal-area construction from DSC experiments ($dT/dt = +10$ K min^{-1}). The ^{13}C NMR spectrum (with $CDCl_3$ as the solvent) shows that the sample is atactic with $78 \pm 4\%$ syndiotactic sequences, corresponding to 60% syndiotriads.

3. Methodical treatment

The rotor-synchronized 2D-MAS exchange measurement was carried out on a Varian UNITY-400 instrument as a combination of a normal and a time-reversal experiment (Hagemeyer *et al* 1989, Luz *et al* 1992, Titman *et al* 1992) giving pure absorptive spectra. We used pulse sequence and phase cycling identical to those used by these authors. A typical experimental time for a series of mixing times at a given temperature was 4–6 days. It should be noted that this method approaches its limits when the rate of the monitored process becomes comparable to the spinning speed. In that case, the spinning side-bands broaden and the signal-to-noise ratio drops. In addition, equation (1) does not hold any longer and a more complicated treatment must be applied (Schmidt and Vega 1987, Kristensen *et al* 1992, Luz *et al* 1993).

In this contribution, only the signal of the carboxyl group (labelled 1 in figure 1) is considered. Owing to the particular position of the carboxyl C atoms between the side and main chains, we expect to see the influence of both the α and β processes. A typical experimental 2D spectrum is shown in figure 2 in comparison to a simulated spectrum. The simulation was carried out using the model proposed for the β process by Schmidt-Rohr *et al* (1994) and Schmidt-Rohr and Spiess (1994). It is obvious that the simulated cross peak intensity is smaller than the experimental results which emphasizes the fact that we have to extend the proposed model to account for the α relaxation.

As chemical exchange does not occur in our polymers and spin diffusion can be excluded (Reichert *et al*), the cross-peaks between various spinning side bands of the COO-line in the 2D-MAS exchange spectra are caused exclusively by molecular reorientations. These reorientations can be detected via the change in the orientation of the anisotropic chemical shift tensor in space and, therefore, the corresponding NMR frequencies. In the 2D NMR exchange experiment these frequencies are compared during the evolution (t_1) and the

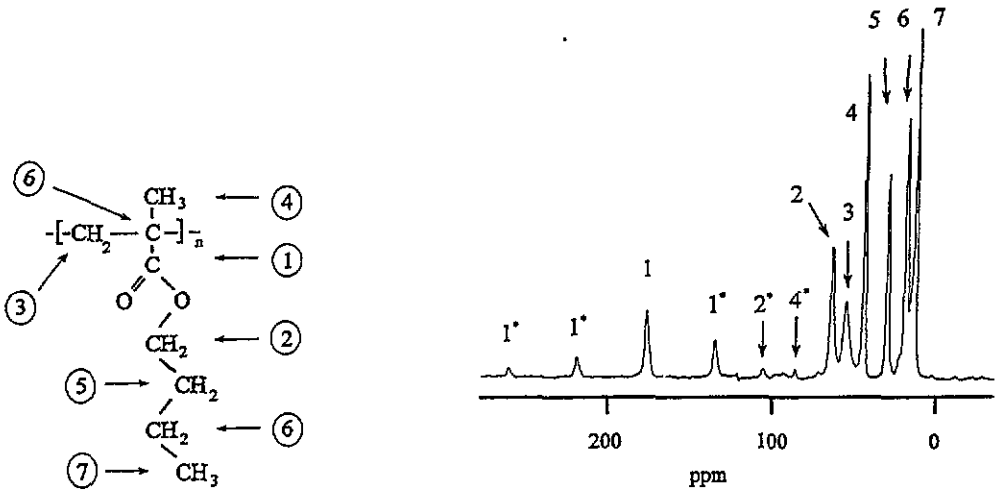

Figure 1. The monomer unit of PnBMA (left) and the ^{13}C CP/MAS spectrum (right); $\nu_{rot} = 4.2$ kHz, $T = 20$ °C. Numbers assign the lines in the spectrum to the different carbons in the monomer unit. (Spinning side bands of the lines belonging to different carbons are marked by asterisks.)

detection (j) times which are separated by the relatively long mixing time τ_m only limited by the generally very long ^{13}C T_1. This method therefore, allows the detection of very slow reorientations. It should be noted that the lower limit of τ_m is the length of few rotor cycles which is of the order of 5 ms for the spinning speed used in our experiments.

We can express the dependence of the intensities for the diagonal ($M = N$) and cross peaks ($M \neq N$) on the mixing time by (Luz *et al* 1992, Titman *et al* 1992):

$$S^{MN}(\tau_m) = \sum_{ij} P_{ij}(\tau_m) I_{ij}^{MN} \exp(-\tau_m/T_1). \tag{1}$$

The I_{ij}^{MN} are being determined exclusively by the geometry of the motional process and depend on the components of the anisotropic chemical shift tensor in the molecular frame and on the tensor transformation, describing the orientation of the carboxyl group relatively to the magnetic field B_0 during the evolution (i) and the detection periods (j) (Luz *et al* 1992). They involve a powder average over the Euler angles relating the molecular frame relative to the rotor axis system. The details of these calculations will be reported elsewhere (Reichert *et al*). Here we are only interested in the time dependence of $S^{MN}(\tau_m)$, i.e. on $P_{ij}(\tau_m)$.

The details of the reorientational process and its timescales are reflected in the fractional population $P_{ij}(\tau_m)$ of the subgroup of those nuclei that have the orientation i during the evolution period and j during the detection period. The $P_{ij}(\tau_m)$ can be obtained from the solution of the kinetic equation (Ernst *et al* 1989) as

$$P_{ij}(\tau_m) = P_i^0 [\exp(\mathbf{K}\tau_m)]_{ij} \tag{2}$$

where P_i^0 is the equilibrium population of site i, and $\mathbf{K}$ is the exchange matrix.

Following a model used in a static multidimensional exchange NMR experiment for PMMA (Schmidt-Rohr *et al* 1994, Schmidt-Rohr and Spiess 1994), we consider a π flip

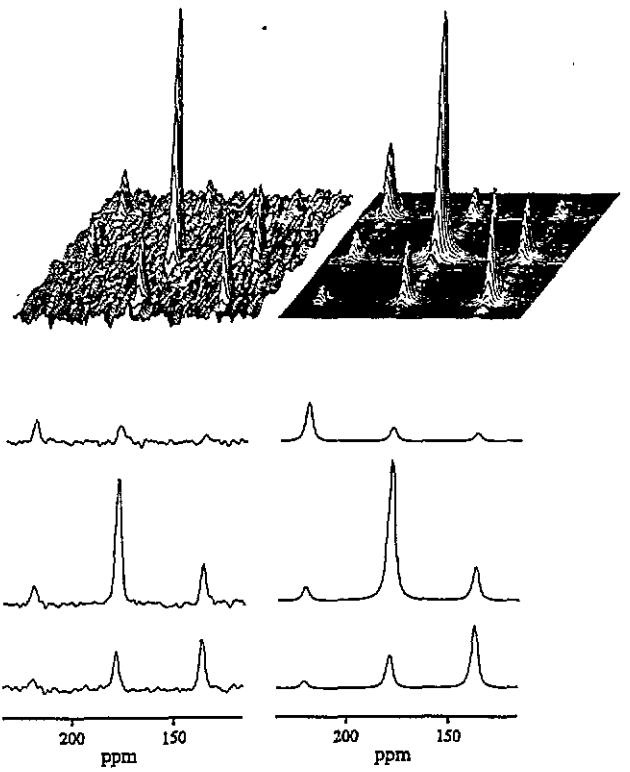

Figure 2. 2D plots (top) and ω_2 traces taken at the peak maxima (bottom): experimental (left) and simulated (right); $T = 20$ °C, $\tau_m = 7$ s, $\nu_{rot} = 4.2$ kHz. The simulation is based on a π flip combined wit a small-amplitude rocking (20°); the eigenvalues of the chemical shift tensor used in the calculation are: $\sigma_{11} = 114.5$ ppm, $\sigma_{22} = 155.6$ ppm, $\sigma_{33} = 264$ ppm. Note that the simulated cross-peak intensities (compared to the intensity of the main-diagonal peaks) are smaller than the experimental intensities.

around C–C bond connecting the main chain and the side group for the side-chain motion, accompanied by a rotation (e.g. about 30°) around the local chain axis (jump ① ↔ ② in figure 3, rate K_f). The second rotation was introduced by the authors mentioned above to avoid steric clashes with the environment during the flip process. We are aware that this model might not be completely correct for PnBMA, owing to the longer side group of PnBMA compared to PEMA. However, since our results are less sensitive to the special geometry of the motional process (see below), it is justified to use this model as probable example. If we further assume: (i) that *any* slow cooperative main-chain motion influences the carboxyl carbon (② ↔ ③ in figure 3, rate K_s); (ii) the possibility of a further flip–rotation combination as described above (③ ↔ ④ in figure 3, rate K_f); and (iii) another slow main-chain motion corresponding to (i) to reach the initial position (④ ↔ ① *in* figure 3, rate K_s), then we have a closed cycle for a four-sites model describing both, main- and side-chain motions. The corresponding exchange matrix **K** is

$$\mathbf{K} = \begin{pmatrix} -K_s - K_f & K_f & 0 & K_s \\ K_f & -K_s - K_f & K_s & 0 \\ 0 & K_s & -K_s - K_f & K_f \\ K_s & 0 & K_f & -K_s - K_f \end{pmatrix} \tag{3}$$

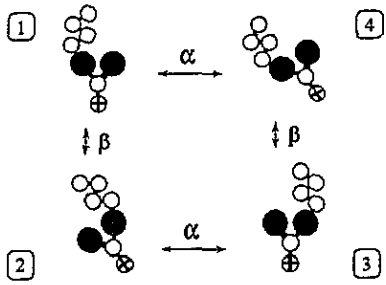

Figure 3. The 'four-sites' model (described in the text); the view on the OCO plane, which is perpendicular to the local main-chain axis ⊗; ①: start position; ① ↔ ②, ③ ↔ ④: combined rotation around the local main-chain axis and π-flip motions: ② ↔ ③, ④ ↔ ①: slow main-chain motion (re-rotation around the local main-chain axis shown here as a possible example).

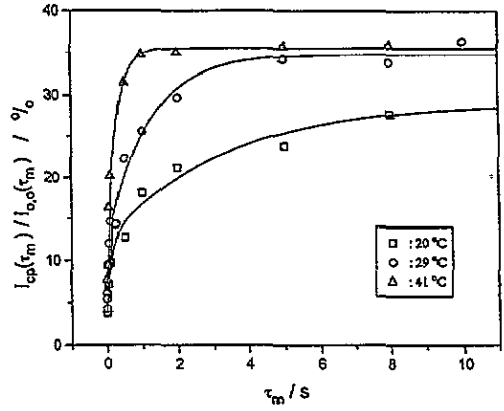

Figure 4. The dependence of the cross-peak intensity ($M = 1$, $N = 0$) on the mixing time (τ_m) for the carboxyl group at different temperatures.

with the exchange rates K_f for the flip combination and K_s for the slow main-chain motion.

For the assignment of K_f and K_s to side- and main-chain motion (i.e. to faster and slower motion) we keep in mind that the proposed flip combination (① ↔ ②, ③ ↔ ④ in figure 3) avoids collisions with the local environment and thus is relatively fast. On the other hand, the motional pathways (② ↔ ③ and ④ ↔ ① in figure 3) require simultaneous motions of the environment, emphasizing the cooperative character of this motion and leading to a much smaller rate K_s. An additional proof for this assignment was found by making use of the high spectral resolution of the MAS technique: the rate constant of the growth of the cross-peaks linking spinning side-bands of main-chain atoms (labelled 3 and 4 in figure 2) is similar to K_s (Reichert *et al*).

Diagonalization of equation (2) can be carried out analytically and gives, with $P_i^0 = 1/4$,

$$P_{ij}(\tau_m) = \frac{1}{16}\sum_{n=1}^{4}(-1)^{(\delta_{1i}+\delta_{1j}+\delta_{n\cdot}+\delta_{nj})}\exp(\lambda_n\tau_m) \tag{4}$$

(δ_{ij} being the Kronecker symbol) with the eigenvalues

$$\lambda_1 = 0 \qquad \lambda_2 = -2K_s \qquad \lambda_3 = -2(K_s + K_f) \qquad \lambda_4 = -2K_f. \tag{5}$$

Therefore, for the dependence of the peak intensities on the exchange time

$$S^{MN}(\tau_m) = \sum_{n=1}^{4} A_n^{MN}\exp(\lambda_n\tau_m)\exp(-\tau_m/T_1) \tag{6}$$

where the A_n^{MN} are linear combinations of the I_{ij}^{MN} according to equations (1) and (4).

For $K_f \gg K_s$ an experimental distinction between λ_3 and λ_4 becomes impossible, i.e. a sum of a positive constant term and two exponential functions with positive (diagonal

peaks) or negative (cross-peaks) prefactors leading to decaying or growing peaks will be observed.

It follows that the measured time constants correspond to the inverse of twice the exchange rates K_s and K_f between the positions under consideration (see equation (5)). This statement also holds true for modified models. If we assume for example that the transitions ① ↔ ④ and ② ↔ ③ in figure 3 are substituted by *any* other slow cooperative main-chain motion, then only the values I_{ij}^{MN} in equation (1), and therefore the prefactors in equation (6), will be changed. However, the exchange rates remain unchanged. This is correct even in the hypothetical case if, owing to the changed main-chain motion, the transition between the orientations ③ ↔ ④ might be impossible (Reichert *et al*). Another modification of the four-sites model described above allows transitions with the exchange rate K_a between the sites ① ↔ ③ and ② ↔ ④ in figure 3. The calculation shows for fast additional exchange ($K_a \approx K_f$) that according to this model only the long exchange rates could be measured. The experiments show in contradiction to this prediction two exchange rates which differ by around one order of magnitude. In the case of slow additional motion ($K_a \approx K_s$), however, both types of motion influence the experimental behaviour with slightly modified interpretation of the time constants.

To give an example of the type of the slow main-chain motions (② ↔ ③ and ④ ↔ ① in figure 3), we assume an additional rotation around the axis normal to the OCO plane and nearly parallel to the local main-chain axis. This motion was proposed to correct the deviation of the side-group arrangement after the flip–rotation combination (① ↔ ② and ③ ↔ ④ in figure 3) from the mirror image of the initial position with reference to the C–C bond connecting the main-chain and the side-group. This kind of motion, which is slow because of hindrances by the environment is represented in figure 3 as a possible realization of the main-chain motion.

The molecular models discussed above should be understood as possible examples. We wish to emphasize that the interpretation of the time constants as the inverse of twice the exchange rates of the two processes is independent of the parameters of the chosen model since modifications of the basic model would lead to a change of the prefactors only.

As can be seen from equations (1) and (6), the time dependence of the peak intensities is also influenced by the longitudinal relaxation time. Therefore, the decay of the peak intensities must be corrected by the T_1 value for the carboxyl carbons, separately measured, or by the use of a ratio which is independent of T_1 (normalization via division by a suitable linear combination of the diagonal and cross-peak intensities). We applied both methods, giving deviations of at most ±30%, mainly because of the large variations of the measured values. This relatively poor precision (corresponding to half a decade) is sufficient, however, for comparison with the shear and dielectric experiment in an Arrhenius diagram.

4. Results and discussion

The cross-peak intensities as a function of the mixing time τ_m for different temperatures are shown in figure 4. The approximate values for K_f and K_s from equations (5) and (6) are given in table 1.

The K_f and K_s rates were transferred to an Arrhenius diagram (Garwe *et al* 1994), also showing the dielectric compliance and shear loss modulus data (maxima of loss peaks for the latter, see figure 5). The two NMR rates fit well to the α and β traces in the splitting region. Moreover, as expected, the NMR rates for the α are near the shear G''_{max} trace, well above the dielectric ϵ'' trace for $T < 35$ °C. This is interpreted in the framework of a

Table 1. Values of the rates K_s and K_f of the slow and the fast processes (see equation (5)). Error limits are standard deviations from the fitting.

T (°C)	20	29	41	46.5
K_s (s^{-1})	0.15 ± 0.05	0.45 ± 0.09	1.7 ± 0.7	1.4 ± 0.5
K_f (s^{-1})	4.2 ± 2.8	20.0 ± 9.6	19.2 ± 8.1	71 ± 20

dispersion law for the α modes (Donth 1992): the modes relevant for both G'' and NMR are at higher frequencies and, therefore, shorter than the α modes responsible for the ϵ'' maximum. A NMR quantity similar to the intensity of dielectric and shear relaxation will be discussed in a forthcoming paper.

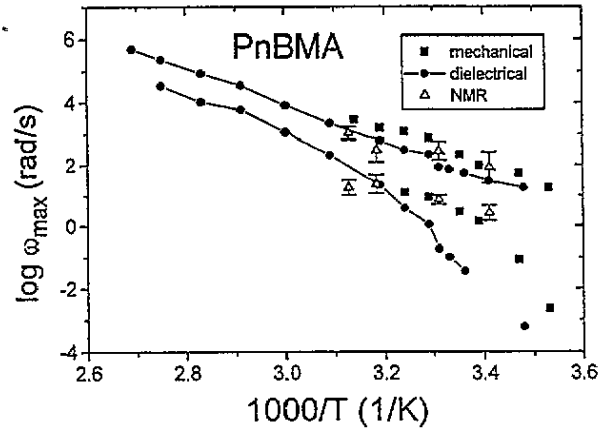

Figure 5. An Arrhenius diagram; characteristic time constants τ_{slow} and τ_{fast} ($\omega_{s,f} = (2\pi/\tau_{s,f})$) compared to mechanical and dielectrical results, ω_{max} = frequency for the G'' and ϵ'' maxima, respectively (Beiner *et al* 1993, Garwe *et al* 1994).

The separate onset of the α-process in the Arrhenius diagram of PnBMA seems to demonstrate that there is no local molecular β precursor for the α process (minimal cooperativity (Donth 1991)). This is different from the scenario in PEMA (Garwe *et al* 1995) where such a local precursor seems obviously to occur (local coordinative β process with unusually high activation energy above the splitting region).

5. Conclusions

The findings of this paper show that the carboxyl carbon (labelled 1 in figure 1) contributes to both the local β relaxation and the cooperative α relaxation in the splitting region of PnBMA in agreement with Kulik *et al* (1994). In addition, we are able to determine rate constants for both relaxation modes. Accepting a dispersion law for the cooperative modes the similarity of G'' and our NMR data in the Arrhenius diagram indicates that the NMR signal reports small-scale molecular mechanisms in accordance with the molecular models of figure 3. It seems that different molecular mechanisms are responsible for the α and β relaxation in PnBMA. Comparing with the molecular simulation with the aid of the Fredrickson model—where both locality and cooperativity are composed from very simple elementary events—we can ask whether the two different mechanisms here could be composed from the same elementary events.

Acknowledgment

The support by the Deutsche Forschungsgemeinschaft (DFG) in the framework of a Graduiertenkolleg is gratefully acknowledged.

References

Beiner M, Garwe F, Hempel E, Schawe J, Schröter K, Schönhals A and Donth E 1993 *Physica* A **201** 72

Donth E 1991 *J. Non-Cryst. Solids* **131–133** 204

—— 1992 *Relaxation and Thermodynamics in Polymers. Glass Transition* (Berlin: Akademie)

Donth E, Schenk W and Ebert A 1979 *Acta Polym.* **30** 540

Ernst R, Bodenhausen G and Wokaun A 1989 *Principles of Nuclear Magnetic Resonance in One and Two Dimensions* (Oxford: Clarendon)

Fedotov V D and Schneider H 1989 Structure and dynamics of bulk polymers by NMR *Methods in NMR—Basic Principles and Progress* vol 21 (Berlin: Springer)

Garwe F, Schönhals A, Beiner M, Schröter K and Donth E 1994 *J. Non-Cryst. Solids* **6** 6941

Garwe F Schönhals A, Lockwenz H, Beiner M, Schröter K and Donth E 1995 *Macromolecules* submitted

Hagemeyer A, Schmidt-Rohr K and Spiess H W 1989 *Adv. Magn. Reson.* **13** 85

Johari G P and Goldstein M 1971 *J. Chem. Phys.* **55** 4245

Kristensen J H, Bilsoe H, Jakobsen H J and Nielsen N Ch 1992 *J. Magn. Reson.* **100** 437

Kulik A S, Beckham H W, Schmidt-Rohr K, Radloff D, Pawezik U, Boeffel C and Spiess H W 1994 *Macromolecules* **27** 4746

Luz Z, Poupko R and Alexander S 1993 *J. Chem. Phys.* **99** 7544

Luz Z, Spiess H W and Titman J J 1992 *Israel J. Chem.* **32** 145

McCrum N G, Read B E and Williams G 1967 *Anelastic and Dielectric Effects in Polymeric Solids* (London: Wiley)

Reichert D, Domberger W and Schneider H 1995 to be published

Schmidt A and Vega S 1987 *J. Chem. Phys.* **87** 6895

Schmidt-Rohr K, Kulik A S, Beckham H W, Ohlemacher A, Pawelzik U, Boeffel C and Spiess H W 1994 *Macromolecules* **27** 4773

Schmidt-Rohr K and Spiess H W 1994 *Multidimensional Solid-State NMR and Polymers* (London: Academic)

Schneider K and Donth E 1986 *Acta Polym.* **37** 333

Schulz M and Donth E 1994 *J. Non-Cryst. Solids* **168** 186

Spiess H W 1991 *Chem. Rev.* **91** 1321

Titman J J, Luz Z and Spiess H W 1992 *J. Am. Chem. Soc.* **114** 3756